# Safe and Adaptive Autonomous Navigation under Uncertainty based on Sequential Waypoints and Reachability Analysis

Nadhir Mansour Ben Lakhal, Lounis Adouane, Othman Nasri, Jaleleddine Ben Hadj Slama

Version of Record: https://www.sciencedirect.com/science/article/pii/S092188902200032X
Manuscript_7d8991680d12ce13743010526b2ffd2f

# Safe and Adaptive Autonomous Navigation under Uncertainty based on Sequential Waypoints and Reachability Analysis

Nadhir Mansour Ben Lakhal[a,b,*], Lounis Adouane[c], Othman Nasri[b], Jaleleddine Ben Hadj Slama[b]

[a] *Institut Pascal, UCA/SIGMA – UMR CNRS 6602, Clermont Auvergne University, 63178 Aubière cedex, France*
[b] *LATIS Lab, National Engineering School of Sousse (ENISo), University of Sousse, BP 264 Sousse Erriadh 1023, Tunisia*
[c] *Université de technologie de Compiègne, CNRS, Heudiasyc UMR 7253, 60203 Compiègne cedex, France*

**Abstract**

This paper presents a new approach for a safe autonomous navigation based on reliable state space reachability analysis. This latter improves an already proposed flexible Navigation Strategy based on Sequential Waypoint Reaching (NSbSWR) framework [1], while considering explicitly different uncertainties in modelling and/or perception. Indeed, NSbSWR is an emergent concept that exploits its flexibility and genericity to avoid frequent complex trajectories' planning/re-planning. The paper's main contribution is to introduce a reachability analysis scheme as a reliable risk assessment and management policy ensuring safe autonomous navigation between the successive assigned waypoints. For this aim, interval analysis is employed to propagate uncertainties influencing the vehicle's dynamics into the navigation system states. By solving an ordinary differential equation with uncertain variables and parameters via an interval Taylor series expansion method, all the vehicle potential reachable state-space is revealed. According to the obtained bounds of the reachable sets, a decision about the navigation safety is made. Once a collision risk is captured, the risk management layer acts to update the control parameters to master the critical situation and guarantee a proper reaching of waypint, while avoiding any risky state. Several simulations results prove the safety, efficiency and robustness of the overall navigation under uncertainties.

*Keywords:* Autonomous navigation, sequential waypoint-based navigation, risk assessment and management, reachability analysis, interval Taylor models.

## 1. Introduction

During the last decades, great progresses have been witnessed in the field of intelligent transportation systems. Efforts have been spent to move towards more reliable and safe navigation approaches. Mobile robots as well autonomous vehicles navigation are generally based on accurate following of references trajectories. In this context, a multitude of sophisticated path planning and/or trajectory computation methods have been practiced [2, 3, 4, 5]. Likewise, several control strategies have been introduced in the literature to track the reference trajectories [6, 7]. However, within the technological advents brought by the community, new challenges have been recently raised for Autonomous Ground Vehicles (AGV) [8, 9, 10]. The ongoing attempts to improve AGV performances have led to complex and computationally demanding trajectory planners. More and more technical constraints must be then satisfied, which complicates the navigation task, mainly in highly dynamic and uncertain environment [11]. Modern AGVs are sensitive to localization and perception inaccuracy. Thus, following precisely a trajectory, while mastering unexpected risks in uncertain and dynamic navigation environments, is not always evident.

### 1.1. Navigation based on waypoints

Offering AGVs an important degree of freedom may be the key solution to face uncertainties and safety challenges. Allowing modern AGVs to act in several possible manners (choose another path, perform different maneuvers, etc.) can provide multiple backup solutions for critical situations. Accordingly, flexibility is now needed as never as a new requirement for AGVs. To address this issue, there is an increasing trend to substitute the conventional trajectory planners by waypoint assignment strategies [12, 13, 14, 15]. Following particular points from a discretized path simplifies drastically the navigation mission. Instead of the arduous path following, few series of waypoints can be properly arranged to guide the vehicle. Contrarily to former approaches, AGVs move freely between the assigned waypoints until reaching a final desired destination.

Currently, the majority of the waypoint following-related work is almost focusing on optimizing this approach performances in terms of stability, traveling time and path smoothness [16, 17]. Safety checking techniques dedicated to this sort of navigation have been roughly linked to obstacle avoidance [18]. Unquestionably, safety verification of the waypoint following approaches requires to be conducted from larger prospects. The appropriate reaching of waypoints under uncertainty is insufficiently investigated. Trajectory re-planning methods with the use of intermediate targets were used in [19]. An error feedback controller was employed to minimize waypoint tracking errors

*Corresponding author:
*Email address:* Nadhir_Mansour.BEN_LAKHAL@etu.uca.fr (Nadhir Mansour Ben Lakhal)

in [20]. Nevertheless, consistency of the adopted error model was not proven. With a posterior knowledge of the navigation environment, a view-matching vision-based approach was utilized to cross the selected waypoints in [21]. Differently in [22], the number and the size of waypoints were reconfigured via a genetic algorithm to reduce the path following errors. According to a Software verification concept, the authors in [23] developed a risk management that checks the temporal and logical behavior of the navigation. Needless to say, Software checking approaches may monitor a limited number of inputs, but cannot deal with the high uncertainty of the navigation dynamics [24].

The lack of safety guarantees for the waypoint-based navigation has profound impacts on its perspectives. Without these warranties, it remains restricted for environments without severe risks. Thanks to its advantages in performing a long-term horizon prediction, Reachability Analysis (RA)[1]has been recently exploited to solve several problems for AGVs, e.g., path parametrization, optimal control and risk identification [25, 26].

### *1.2. Reachability analysis related work*

The considerable available literature on RA has turned this research field into a very active one [27]. On the one hand, the system reachable sets may be revealed via different stochastic models. A particular Probability Distribution Function (PDF) can be selected to rule the transition probability of the system states i.e., the probability quantifying chances of moving from the system actual state to another one. For AGVs, the predicted states via stochastic approaches describes generally vehicles' future occupancy regions [28]. Then, the obtained states are exploited to proceed several tasks from the navigation process, such as localisation, risk assessment, trajectories re-planing, etc. [28]. The polynomial chaos expansion and Markov processes are among the most widespread stochastic techniques used by the AGV community for the aforementioned purposes [29, 30]. However, the reliability of the stochastic RA is still controversial. The definition of a PDF that fits the studied system requires huge amounts of historical data. Moreover, the stochastically derived reachable sets may mismatch reality due to potential changes in the system noise properties [31]. Furthermore, most of the stochastic RA approaches are sensitive to non-linearities of the navigation dynamics [32]. Therefore, huge efforts have been spent to increase these methods confidence. The work reported in [33] employed human-like driving models and empirical data to ameliorate the RA confidence-level to predict behaviors of other drivers and plan safe trajectories for AGVs. Focus has been given also for Monte Carlo multi-simulation to perform reachability for AGVs while assessing the in-road risks [28]. Simultaneous simulation executions of several driving maneuvers with distinct configurations are proceeded. According to the density of the results, occupancy regions of AGVs with the highest prediction probability are pointed out.

As a cut off with the inaccurate stochastic RA, a new wave of set-membership methods have been emerged by relying on the geometrical extrapolation of the system states [34]. Data describing the system variables, inputs and parameters are enclosed into sets to consider the uncertainty e.g., ellipsoids, zonotopes, polytopes, etc. [35]. These sets are propagated through the system model to reveal its reachable space [36]. Using a complex set-representation of data may invoke a considerable computational cost. Although some enclosures are more compact than others (such as zonotopes and ellipsoids), proceeding the computation within these sets is complicated [37]. To simplify the computation through these sets, the studied system linearization is necessary, which entails severe modeling errors. In this regard, the authors in [24] used conservative abstraction methods to deal with the linearization errors impacting the RA performed for AGVs online safety verification.

Rather, extensive research works have been focused on the interval analysis, since intervals are easily handled by formal equations [38]. The reachable sets have been determined via branch and brought interval-based algorithms [39]. The results are accurate, but the recursive nature of these algorithms entails an unpredictable run-time. Another interval-based approaches count on the Differential Inequalities (DIs) that extract tight bounds of reachable sets for the monotonous systems [40]. Therefore, the DI application has been generalized by hybridizing systems into locally monotonous subsystems [41]. The interval Taylor expansion is another interval-based RA approach that may over-approximate a given system reachable states by solving an uncertain Ordinary Differential Equation (ODE) describing the studied system [42]. The system reachable sets are deduced easily by applying a set-integration within whole regions of initial states, inputs and parameters.

In the currently proposed paper, a RA scheme is developed for safety verification of an already proposed flexible Navigation Strategy based on a Sequential Waypoint Reaching (NSbSWR) [1], [12]. All the AGV potential reachable state sets, while moving towards each currently assigned waypoint, are estimated via an interval-based Taylor series expansion. At the best of the authors' knowledge, this is the first proposed risk assessment and management strategy for the NSbSWR with guaranteed performances, since certain predictions are obtained through bounded computation to consider the perception and modeling uncertainties. Not only collision risks can be captured thanks to the proposed method, but also a feedback control solution is applied once a threat is identified. A free-collision reachable space for the AGV future states is obtained by acting on the control parameters.

The rest of this paper is organized as follows: Section 2 describes summarily the NSbSWR architecture and its different components. Section 3 details the proposed RA strategy and validates its consistency through extensive batch simulations. Section 4 presents also the proposed risk management policy based on the obtained RA results and proves its efficiency through simulations. Section 5 concludes this paper and discusses some future works.

[1]RA refers to techniques that pre-estimate the future states of a dynamic system according to its initial states and its potential inputs/parameters [27].

## 2. Overall control architecture for NSbSWR

The target assignment strategy of the tackled NSbSRW was proposed initially in [1]. By allowing performing more maneuvers between waypoints thanks to the NSbSWR flexibility, it is no longer mandatory for AGVs to track precisely a given trajectory. The NSbSWR is also of a great genericity since the navigation turns to a trajectory tracking task when the distance between waypoints is kept short. The proposed work in this paper suggests a novel risk assessment and management level (cf. transparent yellow box in Figure 1) of the studied NSbSWR under high uncertainties. Therefore, there is no intention to detail here the selection of the waypoint configurations i.e., each waypoint's position, orientation and velocity. A high level-planning task is devoted to accomplish this objective [12]. Accordingly, a general overview of the navigation based on waypoints (according to [1, 12]) is given below to understand the NSbSWR main components and to focus later on the principle contribution of this paper. In this sense, the overall control architecture dedicated to deal with such a navigation strategy is illustrated in Figure 1. The main blocks of this architecture are listed below:

- The "Waypoint determination" block (dashed green box in Figure 1) provides the set of appropriate waypoints configuration [12].
- The "Obstacle avoidance" block is activated when an obstacle obstructs the AGV's movement toward its target. The adopted obstacle avoidance method is based on limit-cycle technique which is detailed in [43].
- The "Control law" block guarantees an asymptotically stable reaching of waypoints (cf. Subsection 2.1).
- The "Target assignment" block selects at every sampling step the appropriate target to reach from the set of sequential waypoints (cf. Subsection 2.2).
- The "Reachability analysis" block is responsible of the risk assessment for the NSbSWR. It predicts any potential navigation risks while taking into account several modeling/perception uncertainties (cf. Subsection 2.3).
- The "Adaptive gain" block adapts the control law parameters (gains) to guarantee an appropriate management of risks already captured by the "Reachability analysis" block (cf. Subsection 2.3).

The main components composing the NSbSWR architecture are summarized in the sequel. The main propositions of the paper corresponding to the yellow part given in Figure 1 will be detailed in Section 3 and 4 respectively.

### 2.1. Control law

The waypoints are static targets located in the navigation space. Hence, any asymptotically stable controller can be used for the NSbSWR. The control law adopted in this work showed interesting performances in different autonomous navigation, such as for safe ACC (Adaptive Cruise Control) in [44] and

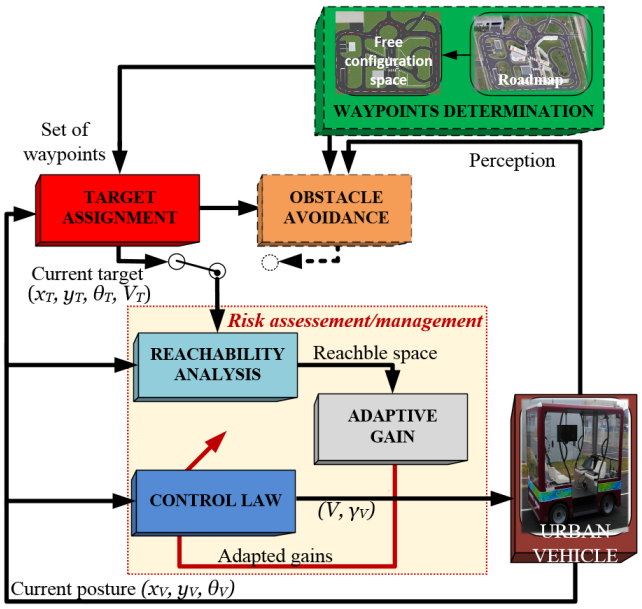


Figure 1: NSbSWR control architecture. The part highlighted in yellow corresponds to the Risk Assessment and Management blocks proposed in this paper.

navigation formation in [45]. Let $(x_V, y_V, \theta_V)$ denote the vehicle posture at a global frame $(O_G, X_G, Y_G)$. Then, a typical tricycle kinematic model is used to describe the vehicle motion:

$$\begin{cases} \dot{x}_V &= V\cos(\theta_V) \\ \dot{y}_V &= V\sin(\theta_V) \\ \dot{\theta}_V &= V\tan(\gamma_V)/l_b \end{cases} \quad (1)$$

where $V$ is the vehicle linear velocity and $\gamma_V$ is its front wheel orientation. $V$ and $\gamma_V$ are the two control inputs of the AGV (cf. equations (5) and (6)). $l_b$ indicates the vehicle's wheelbase. As can be seen from Figure 2, $I_{cc}$ is the center of curvature characterizing the vehicle's trajectory. The curvature and the radius of curvature, which are respectively noted $c_c$ and $r_c$, obey to:

$$r_c = l_b/\tan(\gamma_V) \quad \text{and} \quad c_c = 1/r_c \quad (2)$$

The adopted controller is supposed to lead the AGV towards targets with non-holonomic constraints (cf. Figure 2). Only the target pose $(x_T, x_T, \theta_T)$ and its velocity $V_T$ are needed to perform the navigation. In fact, the control law is synthesized based on the following Lyapunov function $V_L$ (cf. Figure 2):

$$V_L = \frac{1}{2}\left(e_x^2 + e_y^2\right)\left[K_d + K_l \sin^2(e_{VT})\right] + K_o[1-\cos(e_\theta)] \quad (3)$$

where $(e_x,\ e_y,\ e_\theta)$ are the navigation error states with regard to a local frame $(O_L,\ X_L,\ Y_L)$ (cf. Figure 2). $d$ and $\theta_{VT}$ indicate respectively the distance and the angle between the position of the vehicle and the target. $e_{VT} = \theta_T - \theta_{VT}$ is an error variable that identifies the vehicle position-related error while considering the target orientation $\theta_T$. Note that the initial values of $e_{VT}$ and $e_\theta$ must satisfy the following initial conditions:

$$e_{VT} \in \left]-\pi/2, \pi/2\right[ \quad \text{and} \quad e_\theta \in \left]-\pi/2, \pi/2\right[ \quad (4)$$

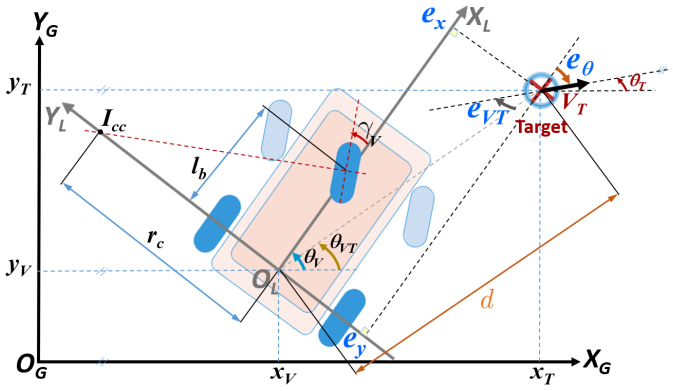


Figure 2: Vehicle/target configurations and control variables

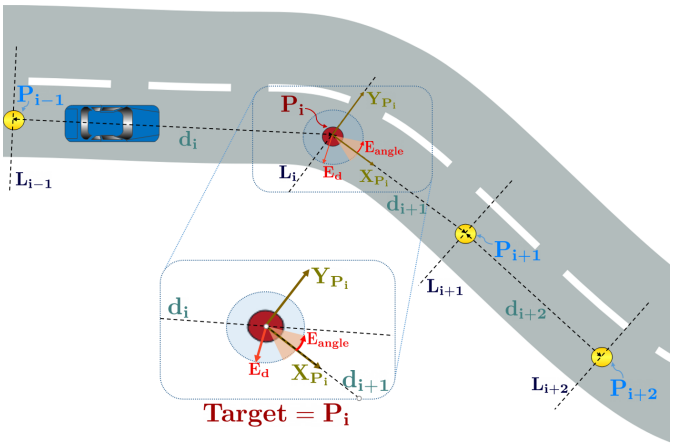


Figure 3: Description of NSbSWR target assignment strategy [1]

The desired linear velocity $V$ and the front wheel orientation $\gamma_V$ of the vehicle which permits to asymptotically stabilize the errors $(e_x, e_y, e_\theta, e_{VT})$ towards zero (allowing therefore to ensure $\dot{V}_L < 0$) are given by:

$$V = V_T \cos(e_\theta) + v_b \tag{5}$$

$$\gamma_V = \arctan(l_b c_c) \tag{6}$$

Afterwards, equations (7) and (8) define $v_b$ and $c_c$ through a set of fixed gains $\mathbf{K} = (K_d, K_l, K_o, K_x, K_{VT}, K_\theta)$:

$$v_b = K_x \left[K_d e_x + K_l d \sin(e_{VT}) \sin(e_\theta) + K_o \sin(e_\theta) c_c\right] \tag{7}$$

$$c_c = \frac{1}{r_{c_T} \cos(e_\theta)} + \frac{d^2 K_l \sin(e_{VT}) \cos(e_{VT})}{r_{c_T} K_o \sin(e_\theta) \cos(e_\theta)} + K_\theta \tan(e_\theta) + \frac{K_d e_y - K_l d \sin(e_{VT}) \cos(e_\theta)}{K_o \cos(e_\theta)} + \frac{K_{VT} \sin^2(e_{VT})}{\sin(e_\theta) \cos(e_\theta)} \tag{8}$$

### 2.2. Sequential target assignment

The strategy to assign, at each sample time, the waypoint to reach by the vehicle is given in Algorithm 1. At every sample time, the relative pose between the vehicle and the target is checked. Then, a decision about whether to keep moving ahead the current target or to shift towards the next waypoint is made. Henceforward, the currently followed waypoint is called target. Let us consider a set of waypoints (cf. Figure 3). Every pair of successive waypoints $P_{i-1}$ and $P_i$ are separated by a distance denoted $d_i$. The orientation of $P_i$, denoted $\theta_{P_i}$, is given by [1]:

$$\theta_{p_i} = \arctan\left(\frac{y_{P_{i+1}} - y_{P_i}}{x_{P_{i+1}} - x_{P_i}}\right) \tag{9}$$

The error conditions, $E_d$ and $E_{angle}$, are used to switch to the next waypoint when the vehicle's position is inside a circle given by the center $(x_{P_i}, y_{P_i})$ and a radius $E_d$. Hence, the current waypoint index is updated with the next waypoint and the vehicle has to adapt its movement according to this new target.

Owing to control imperfections, it is not always possible to lead accurately the vehicle towards the error circle. In such a critical situation, a backup countermeasure must be tackled to carry on the navigation and ensure its liveness. In that case, the local target frame $X_{P_i}Y_{P_i}$ is used. The perpendicular line $L_i$ ($Y_{P_i}$ axis) to the segment relating $P_i$ and $P_{i+1}$ is imposed to guarantee the navigation liveness (cf. Figure 3). Once the vehicle oversteps $L_i$ and the vehicle coordinate $x^{P_i}$ in $X_{P_i}Y_{P_i}$ implies that $x^{P_i} \geq 0$, the switch to the next waypoint should take place.

**Algorithm 1:** Target assignment strategy [1]

**Require:** Waypoints set, vehicle pose, current target $P_i$.
**Ensure :** Sequential switch between waypoints.

```
if (d ≤ E_d and e_θ ≤ E_angle) or x^{P_i} ≥ 0 then
    -Switch to the next waypoint P_i := P_{i+1}.
    -Redefine E_d and E_angle of the new target.
    -Designate a new local coordinate system X_{P_i}Y_{P_i}.
    -Update the vehicle configuration in the new X_{P_i}Y_{P_i}.
end
```

### 2.3. Safety guarantees for target reaching

An analytical method to define the error maximum thresholds $E_d$ and $E_{angle}$, while considering the control law parameters, was presented in [1]. It guarantees the control law ability to guide the vehicle to its current target with error values less than or equal to the derived $E_d$ and $E_{angle}$, while satisfying the vehicle kinematic constraints. The analytical estimation of $E_d$ and $E_{angle}$ given in [1] assumes that the vehicle initial orientation $\theta_{V_0}$ to reach the current target is known with a particular range of uncertainty. Nonetheless, the vehicle dynamics and localization while moving towards the target are supposed as precise. This assumption cannot hold true in case of highly uncertain navigation environments. Due to modeling errors, measurement imprecision and several other disturbances, the assumption made in [1] to consider uncertainties can under-estimate risks endangering the NSbSWR. To consider all uncertainties impacting the navigation process while defining $E_d$ and $E_{angle}$, this paper uses the RA to ensure an appropriate reaching of the target. Compared to the analysis used in [1], a comprehensive online estimation of several modeling/perception uncertainties is included into the NSbSWR framework to ensure the appropriate reaching of waypoints and assess navigation risks.

Aside from the comprehensive estimation of uncertainties to ensure the NSbSWR safety, this work presents another enhancement compared to [1]. Not only the navigation uncertainty-issued threats are captured at an early phase in run-time, but also the control parameters are adapted to overcome these risks (cf. Section 4). Thanks to the adapted controls, the AGV can reach its assigned waypoint while staying always inside the safe/free areas. Together, the RA-based estimation of error boundaries, the analytical relations given in [1] and the proposed strategy to adapt the control parameters build a sound risk management level for the NSbSWR framework.

## 3. Proposed safety verification/management for NSbSWR

In this paper, a novel safety verification and management level for the NSbSWR is introduced. This latter is constructed through two main steps i.e., the risk assessment and risk management strategies (cf. Figure 1). To predict potential navigation in forbidden areas (behind the road limits or regions occupied by obstacles), the RA is exploited to perform the risk assessment. Compared to other RA methods (cf. Subsection 1.2), the Interval Taylor-based RA (ITbRA) provides deterministic results since it does not include any probabilistic prediction. In addition, it uses interval wrappers and does not require any bisection of the system initial states, which offers a valuable simplicity in terms of set-membership calculation and decreases the computational costs [41, 46, 47]. Notably, the interval-based computation suffers from the pessimism issued from the non-compact form of intervals and the absence of correlation assumptions between the interval variables [38]. In this view, the interval Taylor expansion series are known in the literature as an efficient manner to improve the pessimism [38]. Thus, the ITbRA is selected to perform the risk assessment task for the NSbSWR. Afterwards, a methodological manner to adapt the control parameters and master critical situations is proposed to play as a risk management strategy for the NSbSWR.

### *3.1. RA-based risk assessment for NSbSWR*

In this Subsection, the ITbRA set integration method is detailed. Once a waypoint is assigned, the ITbRA process is triggered to calculate the system reachable sets to appropriately assess the maximum uncertainty that may impact the error between the vehicle and the target poses at the arrival time, while introducing the perception and modeling uncertainties. Hence, the evaluated uncertainties in the final arrival states serve to analysis risks about the ability to reach safely the subsequent waypoints.

#### *3.1.1. ITbRA general scheme*

The ITbRA constructs an interval-based model for the studied system while considering uncertainties propagated into its states, initial conditions, controls and parameters. From this scope, the AGV can be described through an uncertain ODE with the following shape:

$$\begin{cases} \dot{x}(t) = f(x,s,p,t) \\ x(t_0) \in [x_0], \quad s \in \mathbb{S}, \quad p \in \mathbb{P} \end{cases} \tag{10}$$

Where $f : \mathbb{R}^n \longrightarrow \mathbb{R}^n$ is a non-linear vector-valued function, which defines the system evolution. Accordingly, $x$ is a finite-dimensional state vector of $n$ interval components $[x_{i=1...n}]$. $x(t_0)$ designates the initial domain, which is assigned to the state vector. $\mathbb{S}$ and $\mathbb{P}$ represent respectively the system control sets and the uncertain domain enclosing the ODE parameters.

Let denote the reachable sets of system (10) during an interval time $[t_0,t_f]$ by $\mathscr{R}(([t_0,t_f];[x_0])$. Notably, $t_0$ is the triggering instant of the RA process. $t_f$ is the satisfaction instant of the waypoint switch conditions (cf. Subsection 2.2) by the reachable sets (the estimated reachable sets are close enough from the waypoint). Notably, $t_f$ cannot be known posteriorly, but it depends on the vehicle velocity and the number of the integration steps that must be proceeded until reaching the target. Thus, the system forward reachable sets $\mathscr{R}([t_0,t_f];[x_0])$ between $[t_0,t_f]$ can be formalized via the ODE solutions issued from system (10) with particular initial condition $[x_0]$ as:

$$\mathscr{R}([t_0,t_f];[x_0]) = \left\{ \begin{array}{c} x(\tau), \quad t_0 \leqslant \tau \leqslant t_f | \\ (\dot{x}(\tau) = f(x,s,p,\tau)) \wedge (x(t_0) \in [x_0]) \wedge (s \in \mathbb{S}) \wedge (p \in \mathbb{P}) \end{array} \right\} \tag{11}$$

Indeed, the form of $\dot{x}(t) = f(x,s,p,t)$ is obtained through a slight modification on the tricycle model given in equation (1):

$$\begin{cases} \dot{x}_V(t) = V cos(\theta_V) + w_1 \\ \dot{y}_V(t) = V sin(\theta_V) + w_2 \\ \dot{\theta}_V(t) = V \dfrac{tan(\gamma_V)}{l_b} + w_3 \end{cases} \tag{12}$$

Where $(w_1,w_2,w_3)^T$ is the vector of interval-type noises that may affect the process. Bounds of the interval components $w_{i=1..3}$ must enclose all possible states of noises e.g., modeling, perception and measurement errors. At this regard, a prior knowledge of these uncertainties is supposed acquired for instance through sensors' features and measurement conditions.

Then, the proposed ITbRA method explores all the possible controls that may be generated within particular uncertain initial states. The min/max bounds of admissible $V$ and $\gamma_V$ are over-approximated via the interval arithmetic. By dealing with set-valued initial states, the interval arithmetic permits to reveal all the admissible controls at every integration step from $[t_0,t_f]$. The target configuration $(x_T,y_T,\theta_T)$ as well as its velocity $V_T$ are assumed as certain. Contrarily, the vehicle pose is henceforth described via interval variables $[x_V],[y_V],[\theta_V]$. Accordingly, $(e_x,e_y,e_\theta,e_{VT},d)$ can be expressed also through intervals (cf. Subsection 2.1). Hence, intervals $[V]$ and $[\gamma_V]$ are given by:

$$\begin{cases} [V] = V_T cos([e_\theta]) + [v_b] \\ [\gamma_V] = arctan(l_b[c_c]) \end{cases} \tag{13}$$

Noticeably, $[v_b]$ and $[c_c]$ are calculated in a set-membership manner by substituting $(e_x,e_y,e_\theta,e_{VT},d)$ by their interval values $([e_x],[e_y],[e_\theta],[e_{VT}],[d])$ in equations (7) and (8). Additionally, $l_b$ (cf. equation 1) is considered as known precisely.

By providing the set-valued controls to the interval Taylor models, $\mathscr{R}([t_0,t_f];[x_0])$ can be obtained iteratively by finding solutions of system (12) at instants $t_i \in [t_0 \ldots t_f]$. Afterwards, solution sets, generated at $t_{i-1}$ starting from $[x_{i-1}]$, are the ODE initial conditions at the next instant $t_i$. The initial conditions should be updated from iteration to another as follows:

$$\begin{aligned} [x_1] &= f([x_0],s,p,t_0) \\ [x_2] &= f([x_1],s,p,t_1) \\ &\vdots \\ [x_i] &= f([x_{i-1}],s,p,t_{i-1}) \end{aligned} \tag{14}$$

Evidently, $[V]$ and $[\gamma_V]$ must be recomputed according to new initial conditions at each $t_i$. The RA process meets its end once bounds of the obtained solution at an instant $t_i$ satisfies the waypoint switch rules (cf. Algorithm 1). Then, the relation $t_f = t_i$ is validated. Suppose that each set solution of equation (12) at $t_i$ is denoted $\mathbb{X}_s(t_i)$. Hence, $\mathscr{R}([t_0,t_f];[x_0])$ is defined as:

$$\mathscr{R}([t_0,t_f];[x_0]) = \bigcup_{t_i=t_0 \ldots t_f} \mathbb{X}_s(t_i) \tag{15}$$

Equation (15) provides a valuable information support about all the future sets that may be occupied by the vehicle. At each integration step, the solutions of $[x_{V_i}]$ and $[y_{V_i}]$ are represented geometrically in the space domain by an axis-aligned box. This latter must consider also the vehicle geometrical shape (the vehicle length and width). Likewise, the vehicle orientation should also be taken into account. Thus, two simple rotations for the obtained box at $t_i$ are realized, where the point $C_i$ ($[mid([x_{V_i}]),\ mid([y_{V_i}])]$) is the rotation center and $\theta_{V_i}$ and $\overline{\theta_{V_i}}$ are respectively the performed rotation angels (cf. Figure 4).

All the vertices of solution boxes of the ODE during $[t_0,\ t_f]$ and those resulting from the rotation are used to bound the vehicle reachable space. A numerically obtained 2D convex hull that encloses all these vertices is used as an envelope of the

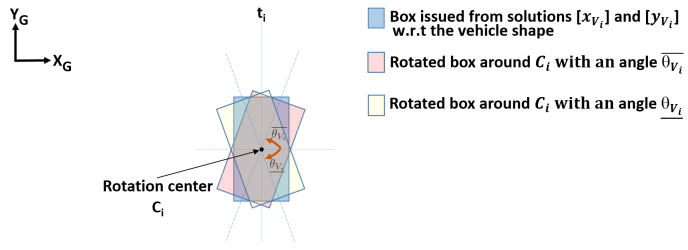


(a) Reachable sets at instant $t_i$

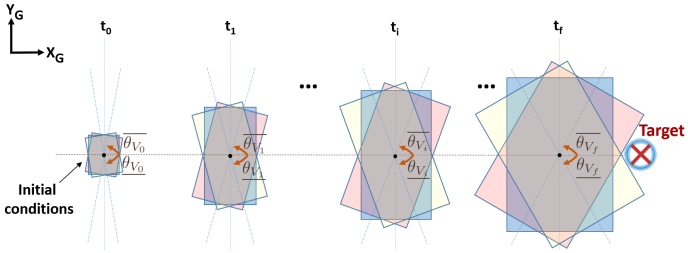


(b) Reachable sets during $[t_0,\ t_f]$ (with initial orientation error $e_{\theta_0} \simeq 0$)

Figure 4: Geometrical representation of reachable sets in the space domain

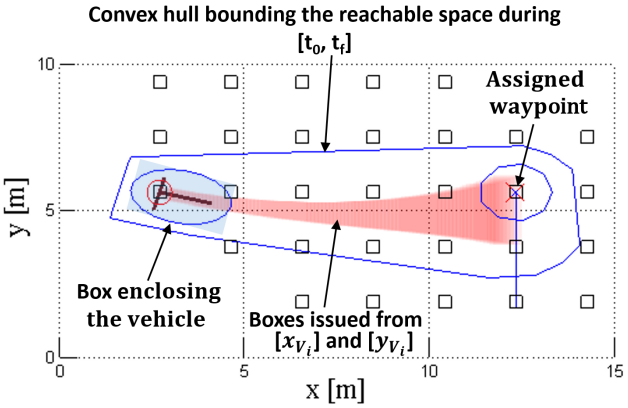


Figure 5: Reachable space bounding through convex hull enclosure

reachable space. In this sense, Figure 5 presents an example of boxes enclosing the ODE solutions as well as bounds of the AGV reachable space while moving towards a given assigned target. Finally, the overall RA proposed for NSbSWR is illustrated in the flowchart shown in Figure 6.

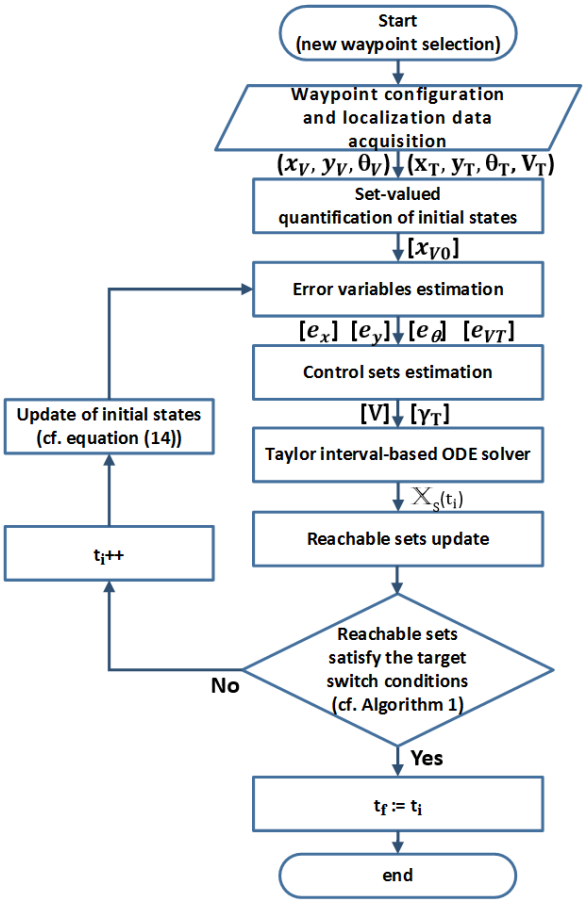


Figure 6: Flowchart of the proposed RA process for reaching a given waypoint

*3.1.2. Standard interval Taylor expansion series*

As explained, the proposed RA is based on interval Taylor expansion applied during a time grid $t_0 < \ldots < t_i < \ldots < t_f$. In general, Taylor set-integration is initiated by looking for a prior enclosure of the set-solution at an instant $t_i$. The prior guess of regions bounding the solutions are not tight enough [41]. Thus, these regions are further refined to obtain the smallest sets bounding the ODE solutions. In fact, obtaining tight bounds of the vehicle reachable space is essential for the safe reaching of waypoints. Conservative values of $E_d$ and $E_{angle}$ will limit the range of possible choices of the waypoints' locations. To avoid huge error boundary values, the distance between the sequential waypoints would be reduced. Such separation distances between the waypoints may be not sufficient enough to fulfill the asymptotic convergence of the navigation errors to zero. Otherwise, important values of $E_d$ and $E_{angle}$ cannot guarantee that the vehicle is always navigating inside the road limits.

Hence, the prior enclosure of the ODE solution, noted $[\hat{x}_i]$, must satisfy the inclusion test in equation (16):

$$\mathbb{X}_s(t) \subset [\hat{x}_i], \quad \forall t \in [t_i, t_{i+1}] \tag{16}$$

During the integration step $\Delta_{t_i} = t_{i+1} - t_i$, the arbitrary guess of $[\hat{x}_i]$ can be realized via the fixed point theorem and the Picard-Lindelö operator [41]. According to these latter, equation (17) approximates a first guess of the prior enclosure that satisfies equation (16) while minimizing the width of $[\hat{x}_i]$ [41]:

$$[\hat{x}_i] = [x_i] + [0, \Delta_{t_i}] f([x_i], [s], p, [t_i, t_{i+1}]) \tag{17}$$

Then, the prior enclosure is recursively tuned until satisfying:

$$[x_i] + [0, \Delta_{t_i}] f([\hat{x}_i], [s], p, [t_i, t_{i+1}]) \subseteq [\hat{x}_i] \tag{18}$$

$\Delta_{t_i}$ can be recursively diminished to satisfy equation (18). Rather, $[\hat{x}_i]$ is iteratively enlarged to proceed with an equally spaced time grid and admit an integration step relative to the AGV sampling time. Once the inclusion of equation (18) is fulfilled, the recursive estimation of $[\hat{x}_i]$ is stopped. The estimated prior enclosure $[\hat{x}_i]$ is still a conservative approximation of the final solution $[x_{i+1}]$. Thus, the over-approximation of $[x_{i+1}]$ is refined with a Taylor expansion of order $k$, as shown in equation (19). Notably, $[\hat{x}_i]$ is employed to assess the interval remainder $r$ and interval Taylor coefficients $f^{(j)}$:

$$\begin{cases} \mathbb{X}_s(t_i) = [x_{i+1}] = [x_i] + \sum_{j=1}^{k-1} \Delta_{t_i} f^{(j)}([x_i], [s], p, t_i]) + r \\ r = \Delta_{t_i} f^{(k)}([\hat{x}_i], [s], p, t_i]) \end{cases} \tag{19}$$

Where $f^{(j)}$ are interval values obtained numerically or through the successive partial derivatives of $f$:

$$\begin{aligned} f^{(0)}([x_i]) &= [x_i] \\ f^{(1)}([x_i]) &= f([x_i]) \\ &\vdots \\ f^{(j)}([x_i]) &= \tfrac{1}{j}\left(\tfrac{\partial f^{(j-1)}}{\partial x} f\right)([x_i]) \end{aligned} \tag{20}$$

To recapitulate the earlier discussed steps, the Taylor set-integration method is described in Algorithm 2.

**Algorithm 2:** Standard interval Taylor method

**Inputs :** $t_i$, $\Delta_{t_i}$, and $[x_i]$.
**Output:** $[x_{i+1}]$.
-Estimate the first guess of $[\hat{x}_i]$ (cf. equation (17)).
**while** $([x_i] + [0, \Delta_{t_i}] f([\hat{x}_i], [s], p, [t_i, t_{i+1}]) \nsubseteq [\hat{x}_i])$ **do**
  -Enlarge the width of $[\hat{x}_i]$.
**end**
-Calculate interval Taylor coefficients (cf. system (20)).
-Calculate the remainder term $r$ (cf. eq. system 19).
-Calculate solution $[x_{i+1}]$:
$[x_{i+1}] = [x_i] + \sum_{j=1}^{k-1} \Delta_{t_i} f^{(j)}([x_i], [s], p, t_i]) + r$

*3.1.3. Complexity analysis*

The computational cost of a single integration step from the interval Taylor method is $O(k^2)$ [41]. Hence, the overall computational complexity of the interval Taylor expansions applied between the interval time $[t_0, t_f]$ is $O(\alpha k^2)$, where $\alpha = \frac{t_f - t_0}{\Delta_{t_i}}$ is the number of the proceeded integration steps (since a constant time integration step $\Delta_{t_i} = t_{i+1} - t_i$ is used). Besides, a second order expansion ($k = 2$) may be sufficient, since the performed RA methodology takes into account the modeling errors through the intervals noises $(w_1, w_2, w_3)^T$ (cf. eq. system (12)).

Furthermore, an apparent advantage of the flexibility offered by the NSbSWR is removing the complexity problems. As soon as a target is assigned via Algorithm 1, the navigation can be carried out with initial values of $E_d$ and $E_{angle}$. Intuitively, these provisional values are obtained based on the analytical analysis depicted in [1] (by only considering the maximum error of the initial conditions of the vehicle position and orientation). Thus, there is more available time to carry on the RA. Once the reachable space prediction is completed, the temporary fixed $E_d$ and $E_{angle}$ can be updated to take into account the uncertainty propagation into the navigation system.

*3.2. ITbRA simulation-based validation work*

An extensive simulation work is undertaken to validate the ITbRA under Matlab. The interval computation is proceeded via the INTLAB package [48]. This interval-based computing environment is selected due to its high portability with Matlab, its provable performances, rigorous results and fast computation [48]. Otherwise, the vehicle reachable sets are represented in the 2D space via a computational geometry toolbox.

To prove the ITbRA consistency through quantitative testes, batch simulations are tackled. To be consistent, the ITbRA findings must always include all possible trajectories of the ODE solutions. The reachable space of a given test configuration is calculated. After that, the vehicle real trajectory is estimated until reaching the chosen target while injecting Gaussian noises into the vehicle state (cf. equation (12)). It allows to verify whether all the vehicle trajectories issued from executions within Gaussian noises are included into the pre-estimated reachability bounds or not. The magnitude of the injected random noises in each sample time cannot exceed the maximum errors attributed to the interval uncertainties used while proceeding

the ITbRA. To deal with the injected stochastic noises during the simulations, an Extended Kalman Filter (EKF) is employed for the AGV localization.

All the simulations presented in this subsection are realized with $V_{max} = 3\ m/s$, $\gamma_{V_{max}} = 20°$ and $V_T = 1\ m/s$. Among numerous realized batch simulations, let us consider a given test scenario where Gaussian uncertainties are injected in the navigation dynamics according to the setups shown in Table 1. To estimate the system reachable space within same minimum/maximum values of stochastic uncertainties, bounds of the interval noises attributed to $(x_V, y_V, \theta_V)$ at every sample time are respectively $\pm 5cm$, $\pm 5cm$ and $\pm 0.5°$.

Table 1: Simulation setups for Gaussian uncertainty injection

| Variable | Minimum | Maximum | Mean | Standard deviation |
|---|---|---|---|---|
| $x_v$ (cm) | -5 | 5 | 0 | 2.5 |
| $y_v$ (cm) | -5 | 5 | 0 | 2.5 |
| $\theta_v$ (°) | -0.5 | 0.5 | 0 | 0.25 |

Including 200 triggered execution, the batch simulation results in the 2-dimensional space are presented in Figure 7. Afterwards, the evolution of $(x_V, y_V, \theta_V)$ obtained via batch simulations and their corresponding reachability-issued frames are illustrated in Figures 8, 9 and 10.

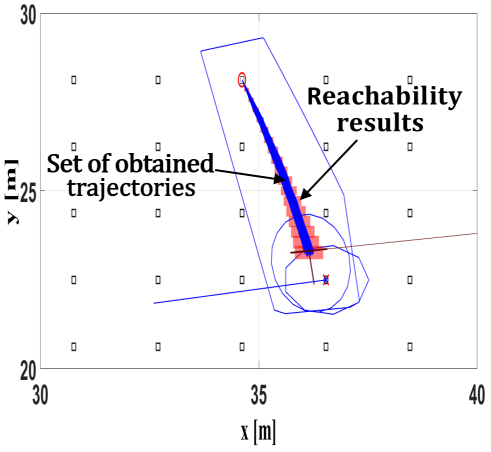


Figure 7: Batch simulation results representation in 2D space

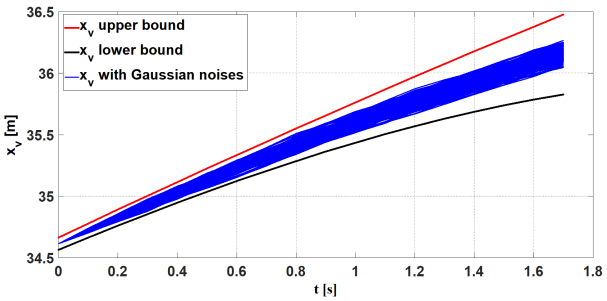


Figure 8: Evolution of $x_V$ compared to reachable space bounds

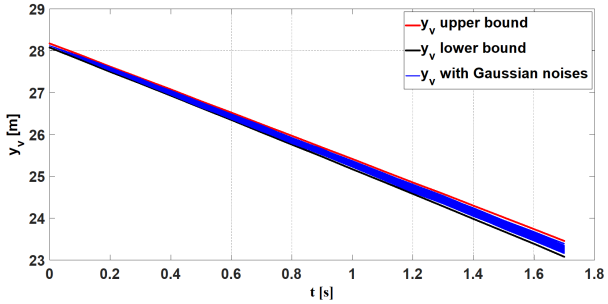


Figure 9: Evolution of $y_V$ compared to reachable space bounds

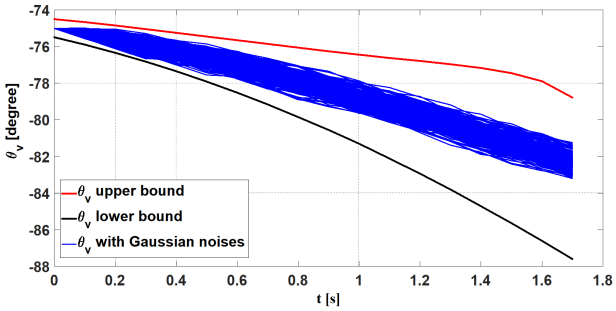


Figure 10: Evolution of $\theta_V$ compared to reachable space bounds

The depicted results prove that the ITbRA-issued bounds enclose perfectly the data obtained via the batch simulations and a successful estimation of the reachable space was undertaken. Thus, the ITbRA reliability in ensuring safety verification for the NSbSWR framework is proved.

## 4. ITbRA-based risk management for NSbSWR

Typically, the use of the RA approaches in the literature is restricted to perform the in-road risk assessment. At the best of our knowledge, this is the first work that establishes a strong link between RA and the control layer to master the predicted risks. The ITbRA outputs are exploited in the sequel to maintain a predefined Lower Distance (LD) to the road limit (or obstacles for certain contexts) as shown in Figure 11.

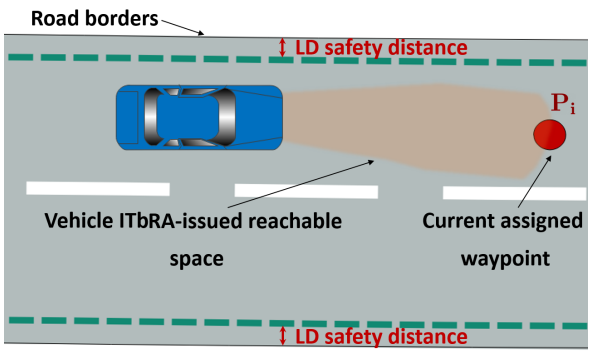


Figure 11: ITbRA-based risk management principle

### 4.1. Proposed risk management algorithm for NSbSWR

As stated earlier, the control stability is guaranteed for all positive parameters $(K_d, K_l, K_o, K_x, K_{VT}, K_\theta)$ [1]. In particular, $K_\theta$ is the parameter influencing on the vehicle angular velocity. Notably, $e_\theta$ is assumed to converge asymptotically towards zero. Through this assumption, equations (6) and (8) imply:

- For $e_\theta \in ]0, \pi/2[$, the term $k_\theta\ tan(e_\theta)$ in equation (8) is positive. Hence, rising $k_\theta$ will deviate the reachable space orientation to the anticlockwise direction (since $\gamma_V = \arctan(l_b c_c) \longrightarrow \pi/2$). Contrarily, if $k_\theta$ drops to zero then the orientation of the vehicle reachable space will move towards the clockwise direction.
- For $e_\theta \in ]-\pi/2, 0[$ and based on the sign of $k_\theta\ tan(e_\theta)$, increasing/decreasing the value of $k_\theta$ will entail respectively the re-orientation of the vehicle reachable space to the clockwise/anticlockwise direction.

Accordingly, the orientation of the AGV reachable space can be changed to always stay in the safe/free areas. The line linking the center of the initial condition box $C_0$ and the center $C_f$ of the reached box at $t_f$ is assumed to outline approximately the direction of the reachable space (cf. Figure 12). As soon as an intersection between reachable state space and forbidden regions is predicted, a new value of $K_\theta$ is selected to guide the AGV to safe zones. Generally, the navigation should be proceeded with the nominal value chosen for $K_\theta$. At instant $t_f$, intersections between the road limits and the AGV reachable space should be verified. If no intersection is found, the nominal value of $K_\theta$ is kept. In the other case, $K_\theta$ is updated until reaching the current assigned waypoint without crossing the forbidden zone. The new $K_\theta$ value aims to rotate the reachable space shape around the center $C_0$ of the initial condition domain with an angle $\theta_R$ to prevent any intersection between the reachable state space and forbidden regions. $\theta_R$ is determined via the angle between the following lines (cf. Figure 13):

- The line crossing $C_0$ and $I_1$, which is the closest point from the road boundary (in intersection with the system reachable space) to the convex shape orientation line.

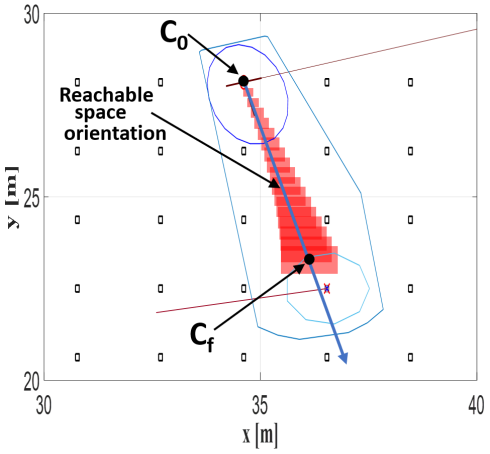


Figure 12: Orientation of the bounded reachable space

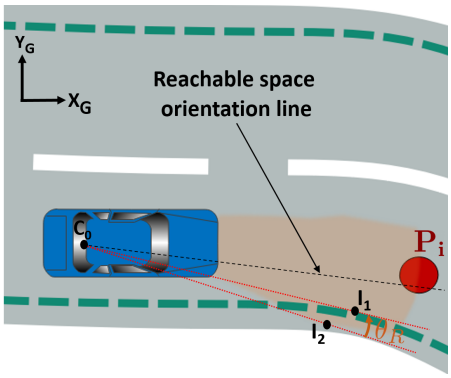


Figure 13: $\theta_R$ estimation method

- The line crossing $C_0$ and the point $I_2$. This latter is the most distant point belonging to the convex hull bound (located behind the road margins) from the road segment in intersection with the road borders.

In practice, the road boundaries may be considered as a poly-line relating points from the borders. Hence, $I_1$ and $I_2$ can be determined via several computational geometry algorithms. The proposed risk management solution can be easily applied to avoid obstacles in the AGV pathway (cf. Subsection 4.2).

In this work, consequences of adapting the nominal value of $K_\theta$ on the reachable space orientation are determined by offline simulations. While using extensive offline tests with large equally spaced values of $K_\theta$, the different changes in the reachable space orientation are stored. According to these results, the most suitable new $K_\theta$ is picked up to achieve the required $\theta_R$. The proposed risk management strategy for the safe reaching of waypoints under uncertainty is summarized in Algorithm 3.

**Algorithm 3:** ITbRA-based risk management strategy

**Require:** Waypoints set, vehicle pose, current target $P_i$.
**Ensure :** Safety guarantees for the NSbSWR.

```
while NSbSWR process is running do
    if new waypoint is assigned then
        -Proceed ITbRA within nominal k_θ.
        -Check collision risks.
        if no collisions are observed then
            repeat
                -Proceed navigation with nominal k_θ.
            until reaching the assigned waypoint
        else
            repeat
                -Estimate θ_R.
                -Adapt k_θ based on the offline results.
            until reaching the assigned waypoint
        end
        -Switch to new waypoint P_i := P_{i+1}.
    end
end
```

Table 2: Waypoints configurations

| | $P_1$ | $P_2$ | $P_3$ | $P_4$ | $P_5$ | $P_6$ | $P_7$ | $P_8$ | $P_9$ | $P_{10}$ | $P_{11}$ | $P_{12}$ |
|---|---|---|---|---|---|---|---|---|---|---|---|---|
| $x_T$ (m) | 9.6 | 13.5 | 19.2 | 23 | 27 | 30.8 | 32.7 | 34.6 | 36.5 | 40.4 | 42.3 | 44.2 |
| $y_T$ (m) | 11.3 | 5.6 | 5.6 | 5.6 | 11.3 | 16.9 | 20.6 | 22.5 | 22.5 | 18.8 | 13.1 | 5.6 |
| $\theta_T$ ($^\circ$) | -55.6 | 0 | 0 | 55.6 | 55.6 | 62.9 | 44.3 | 0 | -44.3 | -71.1 | -75.6 | -90 |

### *4.2. Simulation results*

To prove the efficiency of Algorithm 3, a NSbSWR simulation scenario to cross two sharp road bends is tackled under Matlab. As shown in Figure 14, the risk of crossing the first road deviation is increased by the presence of another vehicle (a static obstacle). The borders represented in grey in Figure 14 are the concrete road limits. The borders drawn in green are the road boundaries after setting a safety distance LD=1 $m$. The vehicle initial pose is: $x_V = 7.8\ m$, $y_V = 16.9\ m$ and $\theta_V = -70^\circ$. A set of twelve waypoints are designated to guide the vehicle. The waypoints' locations are selected in many occasions close to the road borders to invoke critical situations (cf. Table 2). Otherwise, every waypoint's configuration is joined with specific error values to define its own error circle.

At first, the simulation is executed without applying Algorithm 3. The nominal control parameters are maintained all along the navigation run-time, where $K_d = 0.1$, $K_l = 1.8$, $K_o = 60$, $K_x = 0.4$, $K_{VT} = 0.01$ and $K_\theta = 0.19$. The navigation is proceeded with a maximum velocity $V_{max} = 10\ m/s$, a maximum front wheel orientation $\gamma_{V_{max}} = 20^\circ$, and a sampling step equal to 0.02 $s$. All the waypoints' velocities are set to $V_T = 5\ m/s$.

Let denote by $P_i|P_{i+1}$ the period when the vehicle is traveling from the waypoint $P_i$ until reaching $P_{i+1}$. $P_0|P_1$ refers to the travel time between the vehicle initial position and waypoint $P_1$. The extent of interval-type uncertainties injected into the NSbSWR framework to conduct the ITbRA during all periods $P_i|P_{i+1}$ are detailed in Table 3. Remarkably, these extents are attributed to the system initial conditions and noises $(w_1, w_2, w_3)$ (cf. equation (12)). Besides, white noises are injected into the navigation system variables to estimate its real trajectory.

Table 3: Interval-type uncertainty injection setups

| Uncertainty bounds | Periods |
|---|---|
| $(\pm 10cm, \pm 10cm, \pm 0.5^\circ)$ | $P_3\|P_4$, $P_5\|P_6$, $P_6\|P_7$, $P_7\|P_8$, $P_8\|P_9$ |
| $(\pm 10cm, \pm 10cm, \pm 1^\circ)$ | $P_2\|P_3$ |
| $(\pm 15cm, \pm 15cm, \pm 0.5^\circ)$ | $P_4\|P_5$, $P_{11}\|P_{12}$ |
| $(\pm 15cm, \pm 15cm, \pm 0.8^\circ)$ | $P_0\|P_1$, $P_9\|P_{10}$ |
| $(\pm 15cm, \pm 15cm, \pm 1^\circ)$ | $P_1\|P_2$, $P_{10}\|P_{11}$ |

Figure 14a illustrates the overall results of this first simulation scenario in the 2D space domain. The thick green segments in Figure 14a represent the shortest distance separating bounds of the navigation system reachable space and the road boundaries from both sides. These segments approve the safety of the navigation towards the next waypoint. In contrast, the red thick segments underline the regions in intersection with the road safety margins. Accordingly, four potential collisions between the vehicle and the road borders are captured during the simulation run-time. Actually, these collisions are detected respectively during periods $P_2|P_3$, $P_6|P_7$, $P_7|P_8$ and $P_{10}|P_{11}$.

The controller stability is analyzed via the Lyapunov function $V_L$ (cf. equation 3). According to Figure 15, the generated controls are able to ensure the asymptotic stability and the convergence to every waypoint.

Otherwise, Figure 16 exhibits the evolution of the navigation errors in terms of distance to the target and the difference in orientation between the target and vehicle. Accordingly, the proposed control decreases steadily the mentioned errors. Noticeably, the distance to target never reaches zero since the switch between the waypoints is triggered once the vehicle crosses the error circle of a given target.

Then, a second simulation scenario is realized to test the introduced risk management in terms of safety assurance. As shown in Figure 14b, all the collision risks are handled through Algorithm 3. The nominal value of $K_\theta$ was tuned in three occasions (periods $P_2|P_3$, $P_6|P_7$ and $P_{10}|P_{11}$). The earlier captured collision in period $P_7|P_8$ was systematically mastered since the vehicle changed its trajectory during period $P_6|P_7$. Table 4 reveals the applied modification in $K_\theta$ based on the offline results.

Table 4: Risk management modifications in control parameters

| Period | $P_2\|P_3$ | $P_6\|P_7$ | $P_{10}\|P_{11}$ |
|---|---|---|---|
| $\theta_R$ ($^\circ$) | 3.3 $^\circ$ | 8.3$^\circ$ | 3.9$^\circ$ |
| Direction | clockwise | anti-clockwise | clockwise |
| Adapted $K_\theta$ | 0.143 | 0.07 | 0.263 |

The results in Figure 17 confirms the navigation asymptotic stability even within the modification in $K_\theta$. The same shape of the Lyapunov function is obtained compared to the results in Figure 15. Remarkably, the fall in the Lyapunov function during period $P_6|P_7$ ($[7.22s, 8.14s]$) is less important. Indeed, this period witnessed the most important change in $K_\theta$ to enable the required re-orientation angle $\theta_R$. Despite of this change in the Lyapunov function, the NSbSWR stability is still maintained.

Finally, Figure 18 shows the evolution of navigation errors (distance and orientation w.r.t the target). Compared to the first simulation scenario, the performed changes in $k_\theta$ invoked a slight decrease in the convergence rate of $e_\theta$ during $P_2|P_3$ and $P_{10}|P_{11}$. The impacts of the applied modifications on the orientation error $e_\theta$ is more obvious during $P_6|P_7$. Otherwise, the error in terms of final distance to the target is more important than the nominal case during $P_6|P_7$ and $P_{10}|P_{11}$. The realized validation work demonstrated the proposed risk management efficiency. The adopted Lyapunov-based control law

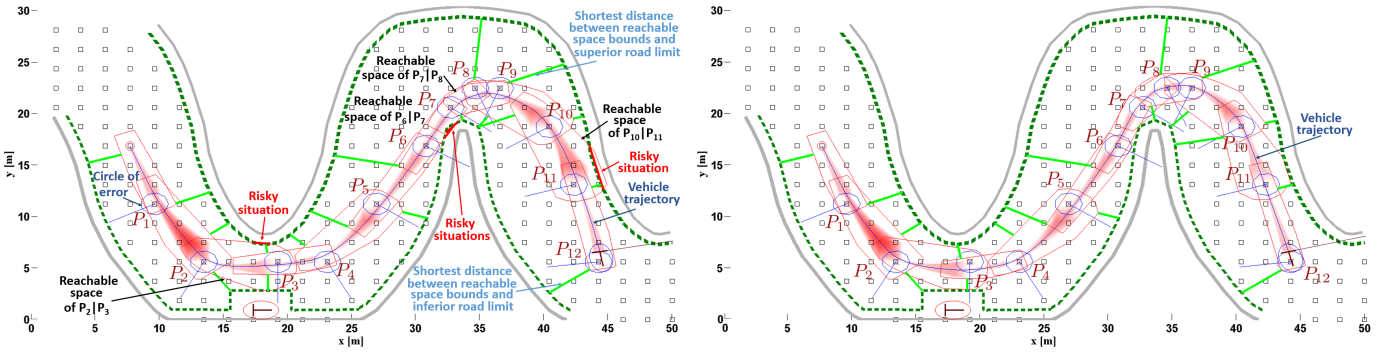


(a) NSbSWR simulation results within nominal control parameters

(b) NSbSWR simulation results within ITbRA-based risk management

Figure 14: Simulations without/without adaptive gain control (available at: `https://bit.ly/2TjP9Gp`)

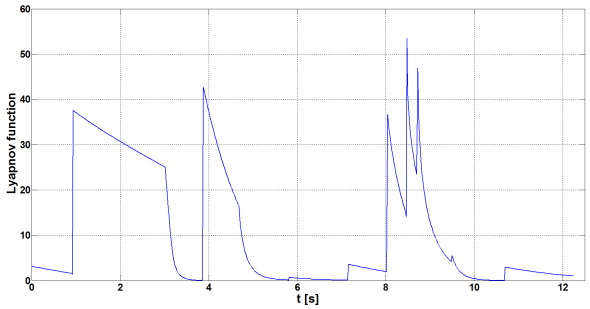


Figure 15: Lyapunov function of adopted control law

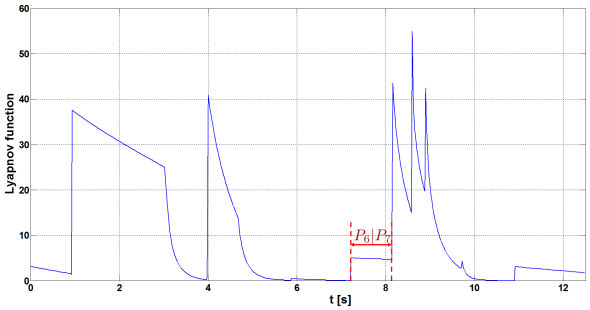


Figure 17: Lyapunov function after adapting the control parameters

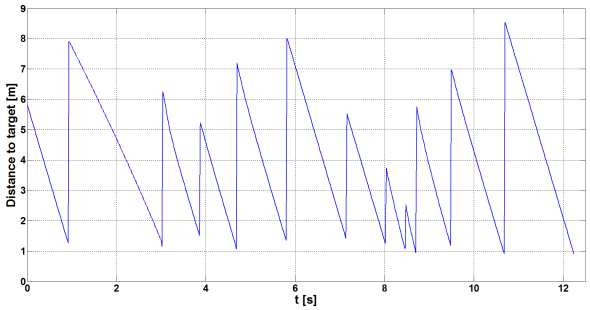


(a) Evolution of distance to current assigned target

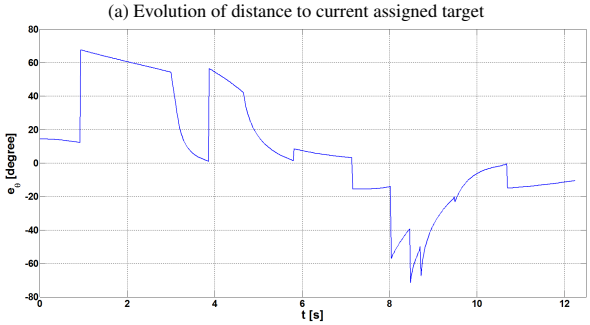


(b) Evolution of angular orientation error

Figure 16: Distance/angular errors with nominal control parameters

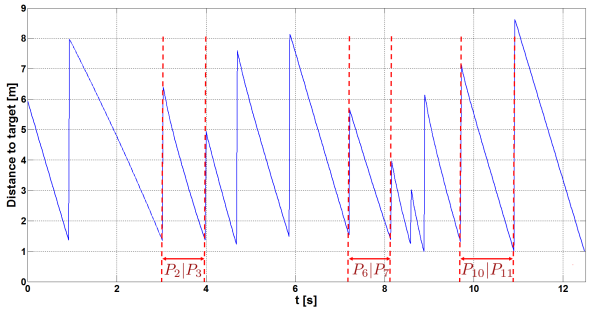


(a) Evolution of distance to current assigned target

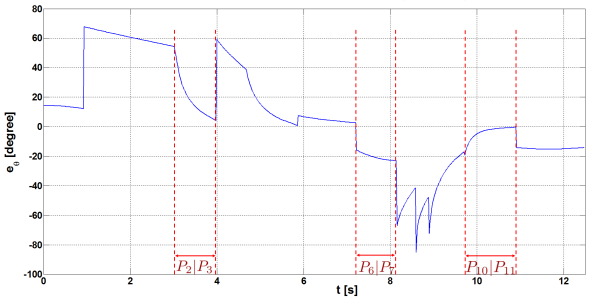


(b) Evolution of angular orientation error

Figure 18: Distance/angular errors with adapted control parameters

maintains always the navigation stability regardless to the value of $k_\theta$ (which must be positive). Safety is guaranteed for the NSbSWR with a harmless loss of precision in the convergence of the navigation system to its target even in worst uncertain case.

## 5. Conclusion

Due to its high flexibility, more attention is paid recently to the Navigation Strategy based on Sequential Waypoint Reaching (NSbSWR) strategies to avoid several trajectory planning/re-

planing complex tasks. In this paper, the interval analysis is used to provide online safety guarantees for a particular NSbSWR strategy. The introduced risk management allows to consider several uncertainties as modeling and perception errors. An uncertain ODE, which describes the navigation according to NSbSWR, is resolved via the interval Taylor method. All potential reachable sets of the navigation future states are revealed. More over, an important link between the control layer and the study of reachability space is established to satisfy the safety requirements. It provides efficient feedback solutions for the NSbSWR once a collision is predicted. Safety is ensured by adapting the control parameters to influence the location of the most probable reachable space and guarantee thus non collision of the vehicle with the forbidden area. The ability of the proposed RA to enclose all possible future states of the navigation under uncertainty is demonstrated via extensive batch simulations. Even more, a convenient simulation scenario was established to test the suggested re-configuration of the adopted controller based on reachability. The simulation results showed that the collision risks have been mastered under uncertainty.

The reachability results should be exploited to define optimal and safe configurations of waypoints in the future. More efficient adaptive control parameters technique should be studied to guarantee a better and faster re-shaping of the vehicle reachable space. Finally, the required technical steps to succeed the implementation of the proposed reachability solution into a real vehicle will be addressed in another future work.

## Acknowledgment

This work receives the support of IMobS3 Laboratory of Excellence (ANR-10-LABX-16-01).

## References

[1] J. Vilca, L. Adouane, Y. Mezouar, A novel safe and flexible control strategy based on target reaching for the navigation of urban vehicles, Robotics and Autonomous Systems 70 (2015) 215–226.

[2] W. Lim, S. Lee, M. Sunwoo, K. Jo, Hybrid trajectory planning for autonomous driving in on-road dynamic scenarios, IEEE Transactions on Intelligent Transportation Systems 22 (1) (2021) 341–355.

[3] O. Sharma, N. Sahoo, N. Puhan, Recent advances in motion and behavior planning techniques for software architecture of autonomous vehicles: A state-of-the-art survey, Engineering Applications of Artificial Intelligence 101 (2021) 104211.

[4] Y. Brouwer, A. Vale, R. Ventura, Informative path planner with exploration–exploitation trade-off for radiological surveys in non-convex scenarios, Robotics and Autonomous Systems 136 (2021) 103691.

[5] L. Adouane, Reactive versus cognitive vehicle navigation based on optimal local and global pelc*, Robotics and Autonomous Systems 88 (2017) 51–70.

[6] X. Di, R. Shi, A survey on autonomous vehicle control in the era of mixed-autonomy: From physics-based to ai-guided driving policy learning, Transportation Research Part C: Emerging Technologies 125 (2021) 103008.

[7] M. W. Mehrez, K. Worthmann, J. P. Cenerini, M. Osman, W. W. Melek, S. Jeon, Model predictive control without terminal constraints or costs for holonomic mobile robots, Robotics and Autonomous Systems 127 (2020) 103468.

[8] Q. Chen, Y. Xie, S. Guo, J. Bai, Q. Shu, Sensing system of environmental perception technologies for driverless vehicle: A review of state of the art and challenges, Sensors and Actuators A: Physical 319 (2021) 112566.

[9] N. M. B. Lakhal, O. Nasri, L. Adouane, J. B. H. Slama, Controller area network reliability: overview of design challenges and safety related perspectives of future transportation systems, IET Intelligent Transport Systems 14 (2020) 1727–1739.

[10] M. Martínez-Díaz, F. Soriguera, Autonomous vehicles: theoretical and practical challenges, Transportation Research Procedia 33 (2018) 275–282, xIII Conference on Transport Engineering, CIT2018.

[11] B. Li, Y. Zhang, Y. Feng, Y. Zhang, Y. Ge, Z. Shao, Balancing computation speed and quality: A decentralized motion planning method for cooperative lane changes of connected and automated vehicles, IEEE Transactions on Intelligent Vehicles 3 (3) (2018) 340–350.

[12] J. Vilca, L. Adouane, Y. Mezouar, Optimal multi-criteria waypoint selection for autonomous vehicle navigation in structured environment, Journal of Intelligent & Robotic Systems 82 (2) (2016) 301–324.

[13] N. Wang, H. R. Karimi, Successive waypoints tracking of an underactuated surface vehicle, IEEE Transactions on Industrial Informatics 16 (2) (2020) 898–908.

[14] A. A. Masoud, A harmonic potential approach for simultaneous planning and control of a generic uav platform, Journal of Intelligent & Robotic Systems 65 (1) (2012) 153–173.

[15] Y. Wang, D. Mulvaney, I. Sillitoe, E. Swere, Robot navigation by waypoints, Journal of Intelligent and Robotic Systems 52 (2) (2008) 175–207.

[16] D. C. Rao, M. R. Kabat, P. K. Das, P. K. Jena, Hybrid iwd-de: A novel approach to model cooperative navigation planning for multi-robot in unknown dynamic environment, Journal of Bionic Engineering 16 (2) (2019) 235–252.

[17] D. Herrero, J. Villagrá, H. Martínez, Self-configuration of waypoints for docking maneuvers of flexible automated guided vehicles, IEEE Transactions on Automation Science and Engineering 10 (2) (2013) 470–475.

[18] C. Sprunk, B. Lau, P. Pfaff, W. Burgard, An accurate and efficient navigation system for omnidirectional robots in industrial environments, Autonomous Robots 41 (2) (2017) 473–493.

[19] H. Cheon, B. K. Kim, Online bidirectional trajectory planning for mobile robots in state-time space, IEEE Transactions on Industrial Electronics 66 (6) (2019) 4555–4565.

[20] W. Gu, S. Cai, Y. Hu, H. Zhang, H. Chen, Trajectory planning and tracking control of a ground mobile robot:a reconstruction approach towards space vehicle, ISA Transactions 87 (2019) 116–128.

[21] P. Nowak, T. C. Stewart, A spiking model of desert ant navigation along a habitual route, in: R. Matoušek (Ed.), Recent Advances in Soft Computing, Springer International Publishing, Cham, 2019, pp. 211–222.

[22] J.-S. Yoon, B.-C. Min, S.-O. Shin, W.-S. Jo, D.-H. Kim, GA-Based Optimal Waypoint Design for Improved Path Following of Mobile Robot, Springer International Publishing, Cham, 2014, pp. 127–136.

[23] D. M. Lyons, R. C. Arkin, S. Jiang, T. Liu, P. Nirmal, Performance verification for behavior-based robot missions, IEEE Transactions on Robotics 31 (3) (2015) 619–636.

[24] M. Althoff, J. M. Dolan, Online verification of automated road vehicles using reachability analysis, IEEE Transactions on Robotics 30 (4) (2014) 903–918.

[25] S. Manzinger, C. Pek, M. Althoff, Using reachable sets for trajectory planning of automated vehicles, IEEE Transactions on Intelligent Vehicles (2020) 1–1.

[26] T. Brudigam, M. Olbrich, D. Wollherr, M. Leibold, Stochastic model predictive control with a safety guarantee for automated driving, IEEE Transactions on Intelligent Vehicles (2021) 1–1.

[27] H. Guéguen, M.-A. Lefebvre, J. Zaytoon, O. Nasri, Safety verification and reachability analysis for hybrid systems, Annual Reviews in Control 33 (1) (2009) 25–36.

[28] M. Althoff, A. Mergel, Comparison of markov chain abstraction and monte carlo simulation for the safety assessment of autonomous cars, IEEE trans Intell Transp Syst 12 (4) (2011) 1237–1247.

[29] J. Suh, H. Chae, K. Yi, Stochastic model-predictive control for lane change decision of automated driving vehicles, IEEE Transactions on Vehicular Technology 67 (6) (2018) 4771–4782.

[30] N. Malone, H. Chiang, K. Lesser, M. Oishi, L. Tapia, Hybrid dynamic moving obstacle avoidance using a stochastic reachable set-based potential field, IEEE Transactions on Robotics 33 (5) (2017) 1124–1138.

[31] J. Nicola, L. Jaulin, Comparison of Kalman and Interval Approaches for the Simultaneous Localization and Mapping of an Underwater Vehicle, Springer International Publishing, Cham, 2018, pp. 117–136.

[32] L. Schafer, S. Manzinger, M. Althoff, Computation of solution spaces for optimization-based trajectory planning, IEEE Transactions on Intelligent Vehicles (2021) 1–1.
[33] K. Driggs-Campbell, V. Govindarajan, R. Bajcsy, Integrating intuitive driver models in autonomous planning for interactive maneuvers, IEEE Trans on Intelligent Transportation Systems 18 (12) (2017) 3461–3472.
[34] N. M. B. Lakhal, L. Adouane, O. Nasri, J. B. H. Slama, Interval-based solutions for reliable and safe navigation of intelligent autonomous vehicles, in: 2019 12th International Workshop on Robot Motion and Control (RoMoCo), 2019, pp. 124–130, Poznań, Poland.
[35] M. Maïga, N. Ramdani, L. Travé-Massuyès, C. Combastel, A comprehensive method for reachability analysis of uncertain nonlinear hybrid systems, IEEE Trans on Automatic Control 61 (9) (2016) 2341–2356.
[36] H. N. V. Pico, D. C. Aliprantis, Reachability analysis of linear dynamic systems with constant, arbitrary, and lipschitz continuous inputs, Automatica 95 (2018) 293 – 305.
[37] T. Nguyen, T. Au, A constant-time algorithm for checking reachability of arrival times and arrival velocities of autonomous vehicles, in: 2019 IEEE Intelligent Vehicles Symposium (IV), 2019, pp. 2039–2044.
[38] L. Jaulin, M. Kieffer, O. Didrit, E. Walter, Applied Interval Analysis with Examples in Parameter and State Estimation, Robust Control and Robotics, Springer, London, 2001.
[39] S. Rohou, L. Jaulin, L. Mihaylova, F. L. Bars, S. M. Veres, Guaranteed computation of robot trajectories, Robotics and Autonomous Systems 93 (2017) 76 – 84.
[40] R. E. Moore, Interval analysis: differential equationsInterval Analysis: Differential Equations, Springer US, Boston, MA, 2009, pp. 1685–1689.
[41] N. Ramdani, N. Meslem, Y. Candau, A hybrid bounding method for computing an over-approximation for the reachable set of uncertain nonlinear systems, IEEE Trans on Automatic Control 54 (10) (2009) 2352–2364.
[42] X. Liao, K. Liu, H. Niu, J. Luo, Y. Li, L. Qin, An interval taylor-based method for transient stability assessment of power systems with uncertainties, International Journal of Electrical Power & Energy Systems 98 (2018) 108 – 117.
[43] J.-M. Vilca, L. Adouane, Y. Mezouar, Reactive navigation of mobile robot using elliptic trajectories andeffective on-line obstacle detection, In Gyroscopy and Navigation Journal, Ed. Springer, Russia ISSN 2075 1087 4 (1) (2013) 14–25.
[44] N. M. B. Lakhal, L. Adouane, O. Nasri, J. B. H. Slama, Risk management for intelligent vehicles based on interval analysis of ttc, IFAC-PapersOnLine 52 (8) (2019) 338–343, 10th IFAC Symposium on Intelligent Autonomous Vehicles IAV 2019.
[45] J. Vilca, L. Adouane, Y. Mezouar, Stable and flexible multi-vehicle navigation based on dynamic inter-target distance matrix, IEEE Transactions on Intelligent Transportation Systems 20 (4) (2019) 1416–1431.
[46] H. Dbouk, S. Schön, Comparison of different bounding methods for providing gps integrity information, in: IEEE/ION Position, Location and Navigation Symposium (PLANS), 2018, pp. 355–366, Monterey, USA.
[47] X. Yang, J. K. Scott, Efficient reachability bounds for discrete-time nonlinear systems by extending the continuous-time theory of differential inequalities, in: Annual American Control Conference, 2018, pp. 6242–6247.
[48] S. Rump, INTLAB - INTerval LABoratory, in: T. Csendes (Ed.), Developments in Reliable Computing, Kluwer Academic Publishers, Dordrecht, 1999, pp. 77–104.

## Biography

**Nadhir Mansour Ben Lakhal** is carrying his research work in robotics and automatic control. His Ph.D is a joint program between Clermont Auvergne University (France) and University of Sousse (Tuinisia). He received his engineering degree in Industrial Electronics in 2014 and his Master's degree in Intelligent and Communicating Systems in 2015 from the National Engineering School of Sousse, Tunisia. He focalizes his research on vehicle/robot safe autonomous navigation and risk management development for intelligent vehicles.

**Lounis Adouane** is a full Professor at Université de Technologie de Compiègne (UTC, France). He received the Ph.D. degree in automatic control from the FEMTO-ST Laboratory, ENSMM, in 2005. During his Ph.D. studies, he deeply investigated the field of mobile multi-robot systems; especially those related to bottom-up and decentralized control architectures. In 2005, he joined the Ampere Laboratory, INSA Lyon, and he studied hybrid (continuous/discrete) control architectures applied to cooperative mobile robots arms. In 2015, he obtained an HDR (habilitation to steer research in robotics) from Blaise Pascal University. From 2006 to 2019, he was an Associate Professor at the Institut Pascal, Polytech Clermont-Ferrand. Currently, Lounis Adouane holds a full Professor position at Heudiasyc, UMR 7253 CNRS / UTC. Between 2018 and 2019, he was the head of ISPR Group (Images, Perception Systems and Robotics, 80 members) at Institut Pascal. Since 2018, Prof. Lounis Adouane is a member of the Technical Committee of IFAC–Intelligent Autonomous Vehicles and serves in the Editorial Board of the Journal of Intelligent and Robotic Systems. Prof. Lounis Adouane is the author/coauthor of more than 120 refereed international papers and two books. His main research interest includes planning and control of mobile robots / intelligent vehicles (autonomous and clean), decision-making under uncertainty, hybrid (continuous/discrete) and hybrid (reactive/cognitive) multi-controller architectures, Lyapunov-based synthesis and stability, cooperative multi-robot systems, artificial intelligence (e.g., MDP or MAS approaches), energy management (e.g., optimal control or neuro-fuzzy approaches).

**Othman Nasri** received the M.S Degree in Control Systems and Applied Informatics from Ecole Centrale de Nantes, France, in 2004, and the Ph.D. degree in automatic control, with emphasis on the safety verification for hybrid systems from Centrale Supelec university of Rennes-France, in 2007. From 2008 to 2010, he was a researcher Engineer in Embedded Control Systems in University of Paris-Sud 11/ INRIA Saclay Île-De-France. He joined the National Engineering School of Sousse and the Laboratory of Advanced Technology and Intelligent Systems, University of Sousse, Tunisia, in 2010. In 2019, he received the Habilitation in electrical engineering from University of Sousse, Tunisia, with emphasis on the supervision and diagnosis of industrial systems. His current research interests revolve around fault detection and isolation techniques, with application to smart systems and autonomous robotics in presence of uncertainty. He works mainly on interval observers, multivariate statistical approaches and reachability analysis.

**Jaleleddine Ben Hadj Slama** (SM'13) received the engineer and the Ph.D. degrees, both in Electrical Engineering, from Ecole Centrale de Lyon, Lyon, France, in July 1994 and December 1997 respectively. Since 2015, he is full Professor in Electrical Engineering at the National Engineering School of Sousse, Tunisia, where he is the leader of the power quality research group in the LATIS laboratory, his main research interests include reliability of transportation systems, Electromagnetic Compatibility (EMC), near-field techniques, EMI issues of power electronics systems and their modeling, Smart Grid, Green datacenters, Renewable Energy and development of remote laboratories for Internet Based Engineering Education.